Chemical Engineering Journal 174 (2011) 436–444

Contents lists available at SciVerse ScienceDirect

Chemical Engineering Journal

journal homepage: www.elsevier.com/locate/cej

Preparation and characterization of mercapto functionalized sepiolite and their application for sorption of lead and cadmium

Xuefeng Liang[a,b], Yingming Xu[a,b,*], Guohong Sun[c], Lin Wang[a,b], Yuebing Sun[a,b], Yang Sun[a,b], Xu Qin[a,b]

[a] Department of Pollution Control, Agro-Environmental Protection Institute of Ministry of Agriculture, Tianjin, 300191, PR China
[b] Key Laboratory of Production Environment and Agro-product Safety of Ministry of Agriculture and Tianjin Key Laboratory of Agro-environment and Food Safety, Tianjin, 300191, PR China
[c] Department of Elementary Science, Tianjin Agricultural University, Tianjin, 300384, PR China

ARTICLE INFO

Article history:
Received 5 July 2011
Received in revised form 23 August 2011
Accepted 23 August 2011

Keywords:
Sepiolite
Mercapto
Functionalization
Characterization
Sorption

ABSTRACT

In order to improve the sorption performance of sepiolite for heavy metals, sepiolite was functionalized by nanotexturization in aqueous sepiolite gel and surface grafting in toluene with mercaptopropyltrimethoxysilane. The pristine sepiolite and mercapto functionalized samples were characterized through XRD, FT-IR, SEM, TEM, TG, surface area analysis, solid state ^{29}Si CP/MAS NMR. The chemical bonding took place between the silanol group within sepiolite and the methoxy group of mercaptopropyltrimethoxysilane. The reaction in aqueous gel produced a continuous coating of individual fibers of sepiolite compared with part grafting on the external surface in toluene. After surface modification, the surface areas decreased due to the bulk size of the mercapto ligand, but the crystal structure did not change obviously, and the stretching of mercapto could be detected by FT-IR. The sorption of Pb(II) and Cd(II) on the samples were studied in batch experiments and it was found that the surface modification can obviously increase the sorption capacities for Pb(II) and Cd(II). The mercapto functionalized sepiolite could provide a potential remedy for heavy metal contamination in soils and water.

1. Introduction

At present heavy metal contamination is one of the widespread environmental problems to jeopardize humans and ecosystem health. The remediation of heavy metal contaminated soil and the treatment of wastewater have become hot topics of environmental science and engineering. Cd, Cu, Pb, Hg, Ni and Zn are considered as the most hazardous metals and listed on the US Environmental Protection Agency's list of priority pollutants. Many techniques have been employed for the treatment of wastewater containing heavy metal ions including precipitation, coagulation, co-precipitation, reverse osmosis, ion exchanges and adsorption.

Among all the different adsorptive materials, clays have been used widely to capture heavy metal ions from aqueous solutions due to their unique properties such as high surface area associated with small particle size, low cost and the ubiquitous occurrence in most soil and sediment environment [1]. Clays can adsorb heavy metal ions through ion exchange or surface complexation [2]. However for natural clay minerals, there are still some limitations such as limited adsorption capacity, relatively small metal binding constants and low selectivity to the type of metals. In the recent years, surface modification of natural clay minerals with reagents containing metal chelating groups have been explored in an effort to enhance the heavy metal binding constants and the selectivity of the type of metals [3,4].

The approaches used for the surface modification of clays include intercalation of organic moieties into the interlayer space, grafting of organic moieties and one step synthesis [5,6]. The intercalation refers to a process that a guest molecule or ion is inserted into the interlayer space by adsorption or ion exchange. The structure of the host and intercalated compound are only slightly changed by the guest species. For instance, four organic-modified clays based on montmorillonite were prepared by embedding ammonium organic derivatives with different chelating functionalities in the interlayer space of montmorillonite as heavy metal ion adsorbents for environmental remediation [7]. Montmorillonite intercalated with poly-hydroxyl Fe(III) complexes was used for the sorption of Cd(II) [8]. Sodium dodecyl sulfate modified iron pillared montmorillonite was applied for the removal of aqueous Cu(II) and Co(II) [9]. Smectite intercalated with non-ionic surfactant has a good performance at removing heavy metal [10]. Grafting is a process that links the inorganic and organic components via strong bonds such as covalent or ionic-covalent to obtain functionalized clays [11,12]. The approach enables a durable immobilization of the reactive organic groups, preventing their leaching when

* Corresponding author at: 31# Fukang Road, Nankai District, Tianjin, PR China. Tel.: +86 22 23618061; fax: +86 22 23006202.
E-mail address: dingandliang@gmail.com (Y. Xu).

1385-8947/$ – see front matter © 2011 Elsevier B.V. All rights reserved.
doi:10.1016/j.cej.2011.08.060

they are used in liquid media. A covalent linkage can be achieved through the reaction between the surface reactive groups and an adequate molecule, which ensures higher chemical structural and thermal stability for the compound. Grafting of amino or mercapto by reaction with the silanol groups onto the surface of clay mineral is of particular interest due to the chelating effect towards heavy metal cations [13,14]. The direct synthesis of hybrid materials having 2:1 phyllosilicate structure has attracted considerable attention. This synthesis route involves in situ incorporation of the organic component during the formation of hybrid material. The silica of the tetrahedral sheets is covalently bonded to the organic groups usually present in the interlayer space. Layered magnesium organosilicates were synthesized for the sorption of heavy metals using several different organosiloxanes [15].

Sepiolite is one of the most suitable clay structures to be grafted with organic moieties due to its high content of silanol groups that are quite easily accessible to the grafting reactants. Sepiolite is a porous and fibrous hydrated magnesium silicate with a large specific surface area (more than 200 m^2/g) with a typical molecular formula of $Mg_8Si_{12}O_{30}(OH)_4(H_2O)_4{\cdot}8H_2O$ from the palygorskite family [16]. Sepiolite structure is composed of blocks of two tetrahedral silica sheets sandwiching an octahedral sheet of magnesium oxide hydroxide [17,18]. Sepiolite has attracted great attention because of its sorptive, rheological and catalytic properties. Through surface modification, the properties of sepiolite can be tailored for specific applications. The structure of sepiolite presents three sorption/modification sites [19]: (a) oxygen ions on tetrahedral sheets, (b) a small amount of cation-exchange sites, and (c) Si–OH groups along the fiber axis.

Great efforts have been made to develop various materials for the remediation of heavy metal pollutions in aquatic and soil environment. However there are limited researches on the surface modification of sepiolite for the remediation of heavy metal pollutions. It is anticipated that the data generated from this work will be useful in the application of functionalized sepiolite in cleanup of metal ions from industrial wastewater and in agriculture.

2. Experiments

2.1. Preparation of mercapto functionalized sepiolite

Pristine sepiolite from Spain (SEP in short), 3-mercaptopropyltrimethoxysilane (MPTMS, >98%) and toluene were purchased from Sigma–Aldrich (China). All the reagents were used as received without any purification. The cation exchange capacity of sepiolite was about 30 meq/100 g.

The surface modification reactions were completed by two approaches: nanotexturization in aqueous gel and surface grafting in toluene. The surface area of pristine sepiolite is about 300 m^2/g and the silanol group density is about 2.2 Si–OH/100 $Å^2$ [20]. The dose of the reagents was set as 1 g MPTMS for 1 g pristine sepiolite.

(1) Nanotexturization. Following the protocol reported by Tiemblo [21], 5 g pristine sepiolite was dispersed in 95 mL water and then was stirred with a lab dissolver (IKA T10 basic ultra-turrax) at 13500 rpm for 5 min to form an aqueous gel. 5 g MPTMS was added to the gel and stirred at 13500 rpm for 15 min. Then all the products were cured in an oven at 100 °C overnight. The product (MSEP-NT in short) was purified by several cycles of washing in dichloromethane and any residual organosilane was removed by Soxhlet extraction over ethanol for 24 h. Finally, all the products were dried at 100 °C for 12 h.

(2) Surface grafting. Sepiolite was functionalized through the covalent grafting of MPTMS by a procedure reported by Mercier [22]. 5 g pristine sepiolite was refluxed for 24 h in 250 mL toluene containing 5 g MPTMS. The mixture was filtered and washed with 250 mL of toluene followed by 250 mL of ethanol. Any residual organosilane was removed by Soxhlet extraction over ethanol for 24 h. The resulting solid (MSEP-GF in short) was recovered by filtration, washed with 100 mL of distilled water, air-dried.

2.2. Characterization of mercapto functionalized sepiolite

The quantitative determination of sulfur content was carried out via elemental analyses in a CNHS analyzer (Vario EL III, Elementar Analysensysteme GmbH). The accessibility of the SH groups in functionalized sepiolite were analysed using Ellman reagent [23]. The method has been adapted from Badyal et al. [24]. It can be used quantitatively because the disulphide within 5,5′-dithiobis(2-nitrobenzoic acid) (Ellman reagent; 99%, Sigma–Aldrich) reacts with the thiol groups bound to sepiolite framework to form an anion which exhibits a strong yellow color absorbing at 412 nm. The absorbance was determined with a UV–vis spectrophotometer (UV-2550, Shimadzu Scientific Instruments). X-ray diffraction (XRD) patterns were recorded on Rigaku D/Max-2500 X-ray diffractometer using Cu Kα radiation at a scanning speed of 1.5°/min over 2θ from 3° to 50° operated at 40 kV and 100 mA. N_2 adsorption desorption isotherm measurements were performed at 77 K with a surface area and porosimetry analyzer (ASAP 2020, Micromeritics Instrument Corp.) in the relative pressure (P/P_0) range from about 10^{-5} to 0.99. The samples were dried and outgassed at 393 K for a minimum of 5 h under vacuum before the N_2 adsorption experiments. The surface area was calculated from adsorption isotherm in the relative pressure range from 0.05 to 0.20. The single-point total pore volume was estimated from the amount of N_2 adsorbed at a relative pressure of approximately 0.98. Micrographs were characterized by LEO 1530VP Field Emission Scanning Electron Microscope (LEO Electron Microscopy Inc.) at an acceleration voltage of 10.0 kV and a working distance of 10 mm at high vacuum mode and JEOL JEM 2010FEF field emission electron microscope operating at 200 kV. The samples were dispersed in ethanol and then deposited on carbon coated copper grids. Infrared spectra were recorded on a FT-IR spectrometer (Magna-IR 560 E.S.P., Nicolet Corp.) in KBr matrix in the range 4000–400 cm^{-1}. Solid state ^{29}Si cross-polarization magic angle spinning nuclear magnetic resonance (CP/MAS NMR) was performed on a Varian Infinity Plus 300 MHz equipped with a 7.5 mm chemagnetics probe in order to determine the covalent bonding of mercaptopropyl group to silicates structure. The NMR experiment was conducted under conditions of magic angle spinning at 3.0 kHz and a 4.5 μs 90° pulse with a repetition delay of 5 s. Chemical shifts have been referenced to the corresponding nuclei in tetramethylsilane (TMS). Thermal characterization of the samples were carried out by thermogravimetric analysis (TGA) on 5 mg samples by heating from room temperature to 800 °C at 10 °C/min, under nitrogen flow (100 mL/min) using a thermobalance (SDTQ600, TA instruments).

2.3. Sorption experiments

Sorption experiments of Pb(II) on pristine sepiolite and mercapto functionalized samples were carried out by the following steps. 0.05 g samples were put into centrifugal tubes, and then filled with $Pb(NO_3)_2$ solutions with different Pb(II) concentrations. The centrifugal tubes were shaking at 25 °C for 24 h in a thermostatic water bath shaker. Then the suspensions were centrifuged at a speed of 13,000 rpm/min. The supernatants were collected to determine the equilibrium Pb(II) concentrations by atomic absorption spectrometer (Solaar M6, ThermoElemental). The equilibrium sorption amounts were calculated from the decreases of Pb(II) con-

centrations. The sorption experiments of Cd(II) on sepiolite samples were done in the same methods and procedures.

3. Results and discussion

3.1. Preparation of mercapto functionalized samples

Sulfur content was calculated from the elemental analyses data and the results were 3.83 and 1.72 mmol/g for MSEP-NT and MSEP-GF. The elemental analyses data provided the total loading of mercapto groups in the functionalized solids regardless of where the mercapto functionality was located, either exposed on the surface or buried within the framework [25]. However, only chemically accessible mercapto functional groups on the surface are quantified in the Ellman reagent methods. The accessible mercapto contents determined by Ellman reagent were 1.59 and 0.87 mmol/g for MSEP-NT and MSEP-GF respectively. The results suggest that a larger fraction of the mercapto groups are accessible in MSEP-NT than in MSEP-GF and are therefore available for applications such as heavy metal extraction from solution. The difference in the mercapto contents suggested that in the same reagents dose, the reaction in aqueous gel is more effective than that in toluene. Toluene is not able to break down the sepiolite aggregates into small bundles or isolated fibers. Only traces of water from sepiolite are present in the toluene suspensions so that hydrolysis and condensation of the silane are much slower and less complete [26]. In term of operating simplicity and large scale production, nanotexturization is better than surface grafting in toluene.

3.2. Characterization of pristine sepiolite and mercapto functionalized samples

The XRD patterns of pristine sepiolite and mercapto functionalized samples are shown in Fig. 1. Sepiolite shows an orthorhombic crystalline system with a space group *Pncn* and the XRD indexes are listed in Table 1. The characteristic diffraction peak was found in all the three diffraction patterns at about $2\theta = 7.3^\circ$ (1 1 0), corresponding to the internal channel reflections [27]. The mineral sepiolite $Mg_4Si_6O_{15}(OH)_2{\cdot}6H_2O$ (JCPDS card No. 13-0595) was detected by Jade 5.0. The characteristic peak positions and *d*-spacing of samples did not change obviously after surface modification with MPTMS, indicating that the structure and crystallinity of sepiolite were maintained in the mercapto functionalized samples because MPTMS functionalization occurred mainly on the surface or by partial replacement of zeolitic water [28]. Compared with pristine sepiolite, the diffraction intensity of mercapto functionalized samples decreased, which could be contributed to the formation between silanol group on the surface of sepiolite and methoxy groups attached to the Si–O matrix. The *d*-spacing of sepiolite was hardly influenced by organic modifier. However, the surface modification could decrease the aggregation of fibers and result in a weak diffraction peak, because the layers of sepiolite were linked by covalent bonds, which were different from the layers of montmorillonite by the faint Van der Waals force [29]. The diffraction intensity of MSEP-NT was the least in the three diffractograms because of the formation of a 3D network of sepiolite fibers at high shear speed [21]. Surface modification by the processes of impregnation or suspension in organic solvents, was produced on the external surface of the sepiolite aggregates, since highly hydrophilic sepiolite was not finely dispersed in these solvents.

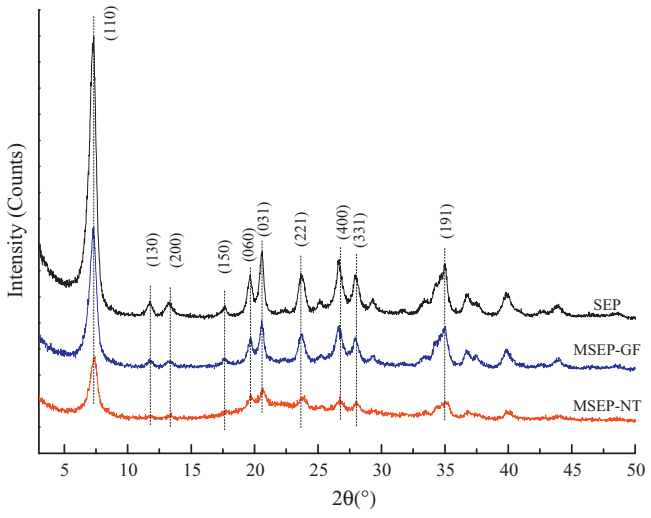

Fig. 1. XRD patterns of pristine sepiolite and mercapto functionalized samples.

The substitution of silanol groups on the surface of pristine sepiolite by the larger mercapto silane groups should have produced changes in the texture of these fibrous clays. This effect was indicated by the results of N_2 adsorption desorption isotherms. As shown in Fig. 2, all the isotherms represented type IV isotherm with a narrow H4 type hysteresis loop according to the IUPAC classification [30], which is a typical curve in mesoporous solids. For pristine sepiolite, the BET surface area of 304.57 m^2/g and total pore volume of 0.48 cm^3/g were determined by BET method. After surface modification, the surface area decreased to 62.79 and 84.78 m^2/g for MSEP-NT and MSEP-GF, respectively. The mercapto functionalization caused a significant decrease in the surface area due to the bulk size of the mercapto ligand which blocked the entrance to some structural channels [20,31]. Despite the reduction in surface area after functionalization, the considerable surface area retained by MSEP-NT and MSEP-GF suggested that the mercapto functionalities were relatively accessible for heavy metal ion binding.

Three regions indicative for sepiolite were observed in Fig. 3 [32]: bands in the 4000–3000 cm^{-1} range corresponding to the vibrations of the Mg–OH group [33], bound water coordinated to magnesium in the octahedral sheet and zeolitic water in the channel, which suggested that the surface of sepiolite fibers was covered by a compact layer of zeolitic and adsorbed water [34,35];

Table 1
XRD indexes of pristine sepiolite and mercapto functionalized samples.

h k l	SEP			MSEP-NT			MSEP-GF		
	2θ (°)	Height	*d* (Å)	2θ (°)	Height	*d* (Å)	2θ (°)	Height	*d* (Å)
(1 1 0)	7.320	2573	12.0672	7.321	924	12.0656	7.320	1204	12.067
(0 6 0)	19.640	379	4.5163	19.679	173	4.5075	19.702	165	4.5022
(0 3 1)	20.599	590	4.3083	20.622	249	4.3036	20.561	330	4.3160
(2 2 1)	23.661	362	3.7571	23.759	188	3.7418	23.718	263	3.7482
(4 0 0)	26.660	419	3.3409	26.760	155	3.3287	26.680	286	3.3384
(1 9 1)	34.980	464	2.5630	35.119	183	2.5531	35.040	361	2.5588
a			13.3636			13.3148			13.3536
b			27.0978			27.045			27.0132
c			4.9018			4.8977			4.9177

Table 2
Summary of selected IR data and assignments of pristine sepiolite and mercapto functionalized samples.

Assignment	Wavenumber (cm^{-1})		
	SEP	MSEP-NT	MSEP-GF
Mg–OH	3689.65; 690.77; 654.59	3689.17; 691.33; 646.03	3688.62; 691.07; 647.44
$H_2O_{coordinated}$	3566.20	3563.83	3563.90
$H_2O_{zeolitic}$	3421.20; 1663.20	3429.99; 1659.87	3415.93; 1663.81
$C–H_{–O–CH3}$	–	2930.43	2932.59
SH	–	2556.22	2562.66
Si–O	1212.52; 1079.00; 978.66	1212.31; 1080.36; 979.66	1210.59; 1078.54; 980.17
Si–O–Si	1019.36; 471.78	1022.92; 470.69	1019.45; 470.72
Si–O–Mg	440.49	440.46	441.31

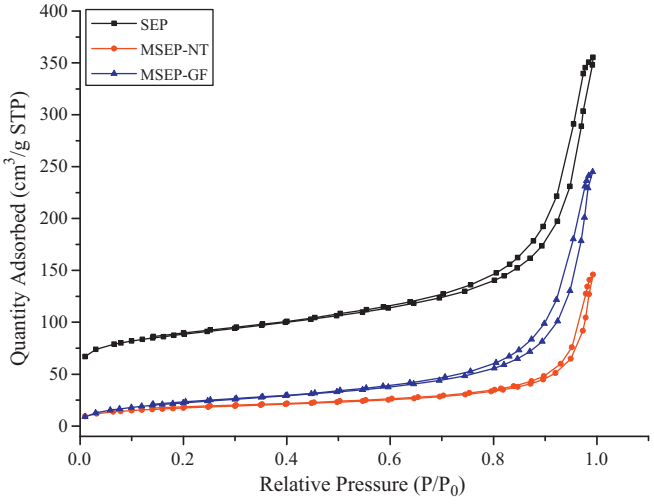

Fig. 2. N^2 adsorption–desorption isotherms of pristine sepiolite and mercapto functionalized samples.

a band at 1663.20 cm^{-1} due to the bending of zeolitic water; bands in the 1200–400 cm^{-1} range characteristic of silicate; bands centered at 1019.36 and 471.78 cm^{-1} due to stretching vibrations of Si–O–Si groups of the tetrahedral sheet; bands at 1212.52, 1079.00 and 978.66 cm^{-1} due to Si–O bonds [36]; a band at 440.49 cm^{-1} originating from octahedral–tetrahedral bonds (Si–O–Mg bonds) and bands at 690.77 and 645.99 cm^{-1} corresponding to Mg–OH bond vibrations [37,38]. The FT-IR spectra of mercapto functionalized samples were generally similar to that of pristine sepiolite and the summary of selected IR data and assignments are listed in Table 2.

For MSEP-NT, the peaks due to the C–H stretching vibration of chain methylene ($–CH_2–$) groups at 2930.43 cm^{-1} and stretching vibration of mercapto group at 2556.22 cm^{-1} were clearly seen and these for MSEP-GF appear at 2932.59 and 2562.66 cm^{-1} respectively [39]. Since there was no C–H bond on pristine sepiolite, the change in the C–H vibrations in the mercapto functionalized samples was the best evidence for the modification of MPTMS.

Solid state ^{29}Si CP/MAS NMR has been shown to be a reliable method in previous references for quantitatively characterizing the nature of various solid surfaces. Regardless of the materials series and their mercaptopropyl group loading, distinct resonances characteristic of siloxane [$Q^n = Si(OSi)_n(OH)_{4-n}$, $n = 2–4$] and organosiloxanes [$T^m = RSi(OSi)_m(OH)_{3-m}$, $m = 1–3$] species could be observed [40]. The results of sepiolite and mercapto functionalized samples are shown in Fig. 4. For pristine sepiolite, the spectrum consisted of four well-resolved resonances. Three main resonances at −92.2, −94.6 and −98.2 ppm have been attributed to the three pairs of equivalent Si nuclei in the basal plane. Resonance at −92.2 ppm was attributed to Si atoms near the edge, −94.6 and −98.2 ppm

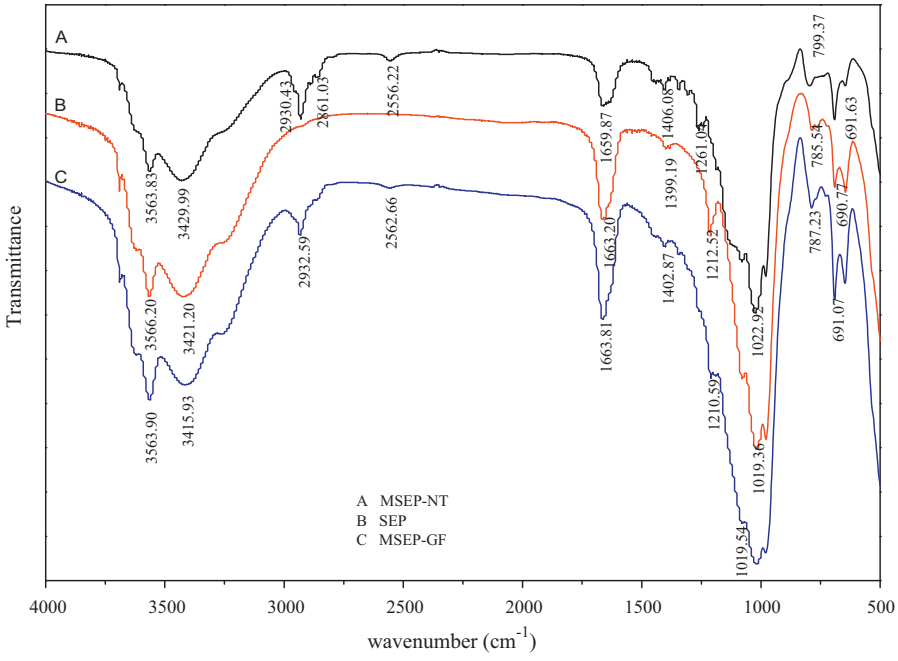

Fig. 3. FT-IR spectra of pristine sepiolite and mercapto functionalized samples.

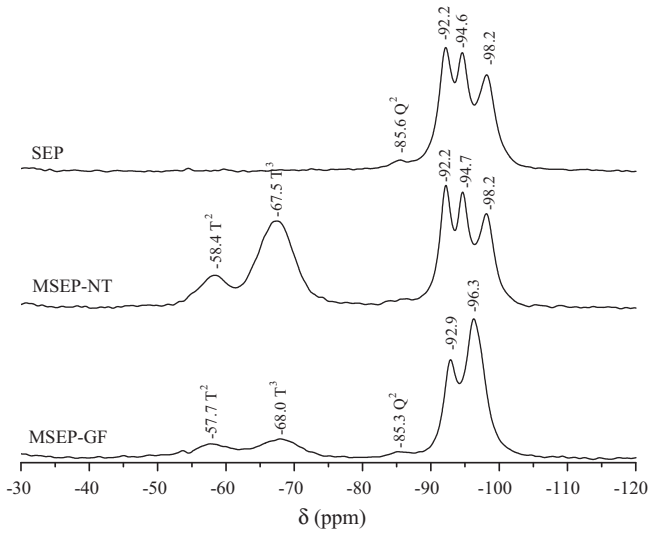

Fig. 4. ^{29}Si CP/MAS solid state NMR spectra of pristine sepiolite and mercapto functionalized samples.

signals to Si atoms sited at the center and the edge of structural blocks respectively [41–44]. The resonance at −85.0 ppm was attributed to Q^2 ($Si(OH)_2$) silanol atoms sited at the borders of the external surface of pristine sepiolite [45].

New resonances for T^2 ($RSi(OSi)_2(OH)$) and T^3 ($RSi(OSi)_3$) were detected at about −58 ppm and −68 ppm in mercapto functionalized samples respectively. The intensity ratio T^3 to T^2 signals was larger for MSEP-NT ($T^3/T^2 = 5.26$) than MSEP-GF ($T^3/T^2 = 2.54$), indicting that condensation was higher and hydrolysis was more complete in aqueous gel nanotexturization [46,47]. The intensity ratio of the inorganic sepiolite signals (*Q* region) to the organic silane signals (*T* region) was higher in MSEP-GF than in MSEP-NT. The Q^2 signal was absent in MSEP-NT and significantly reduced in MSEP-GF in comparison with pristine sepiolite.

Q spectral region in MSEP-GF presented two single signals in comparison with the three *Q* signals observed in MSEP-NT. The merging of two of the *Q* signals has been observed in dehydrated sepiolite [48], where zeolitic water has been removed by thermal treatments similar to those used to dry the samples in this work.

As shown in Fig. 5(A), pristine sepiolite was composed of elemental particles with needle-like of fiber-like shape. Individual needles were generally assembled in bundles of fibers few microns long and about 200 nm thick. The interactions between nanofibers formed dense aggregates with 10–30 μm in size for the pristine sepiolite. For MSEP-NT, after high speed shear, the fibers appeared disaggregated as almost individualized units to form a 3D network of sepiolite fibers. For MSEP-GF, sepiolite agglomerates covered by organic modifier were found. Many single fibers could be observed clearly in both functionalized samples but most of the fibers retained a strong interaction between them after the modification process.

The TEM micrographs in Fig. 6 showed the pristine sepiolite fibers having needle morphology of 30–50 nm in diameter and 1–5 μm in length. These fibers formed bundles-like aggregates by surface interaction between individual needle-type particles. Large fibers were observed but they were formed by connected fibers as confirmed by detailed observation of disperse single sepiolite fibers. After surface modification, the functionalized samples presented also needle morphology. For MSEP-NT, the surface of sepiolite fibers was covered with condensed MPTMS discrete spheres of about 20 nm in diameter [21]. However for MSEP-GF, the borderline of the fibers looked irregular, likely due to the grafted organic molecule.

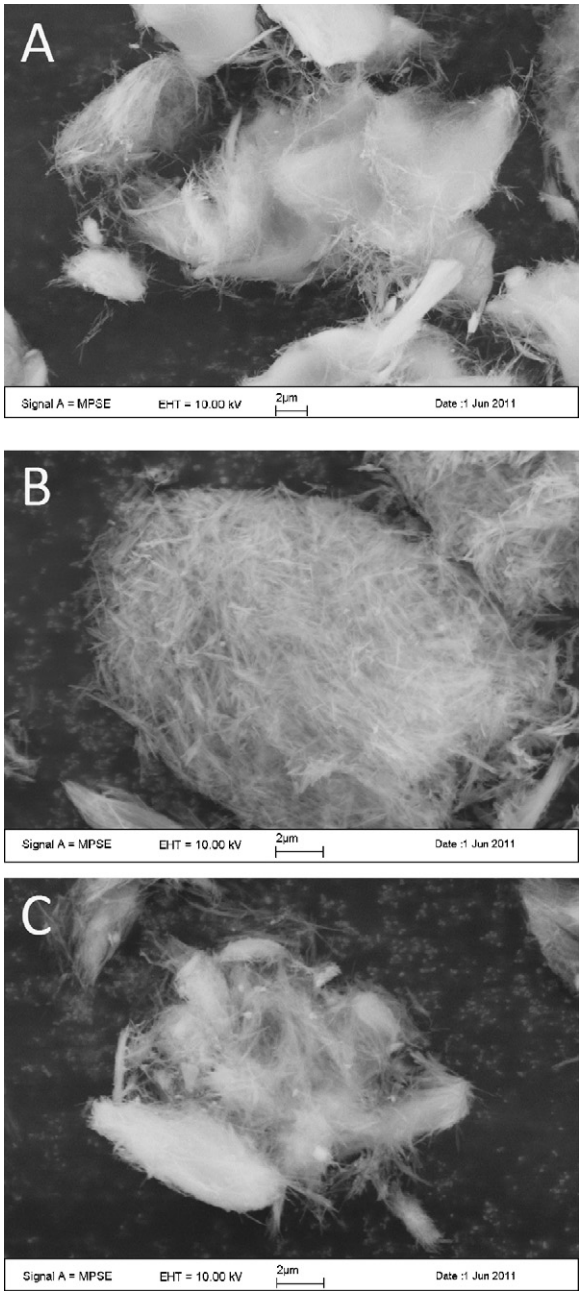

Fig. 5. SEM micrographs of pristine sepiolite and mercapto functionalized samples. (A) SEP; (B) MSEP-NT; (C) MSEP-GF.

The thermogravimetric and derivative thermogravimetric curves of pristine sepiolite and mercapto functionalized samples are shown in Fig. 7. Different weight losses were detected and the data were summarized in Table 3.

The reactions of pristine sepiolite during heating can be summarized as follows [49,50]:

Step 1 $Mg_8Si_{12}O_{30}(OH)_4(H_2O)_4{\cdot}8H_2O \rightarrow Mg_8Si_{12}O_{30}(OH)_4(H_2O)_4 + 8H_2O$

Step 2 $Mg_8Si_{12}O_{30}(OH)_4(H_2O)_4 \rightarrow Mg_8Si_{12}O_{30}(OH)_4(H_2O)_2 + 2H_2O$

Step 3 $Mg_8Si_{12}O_{30}(OH)_4(H_2O)_2 \rightarrow Mg_8Si_{12}O_{30}(OH)_4 + 2H_2O$

Step 4 $Mg_8Si_{12}O_{30}(OH)_4 \rightarrow 8MgSiO_3 + 4SiO_2 + 2H_2O$

The TG curves revealed that the burn out of the mercapto modifier predominated in addition of the sepiolite weight losses. The first weight loss near 100 °C was ascribed to zeolitic water

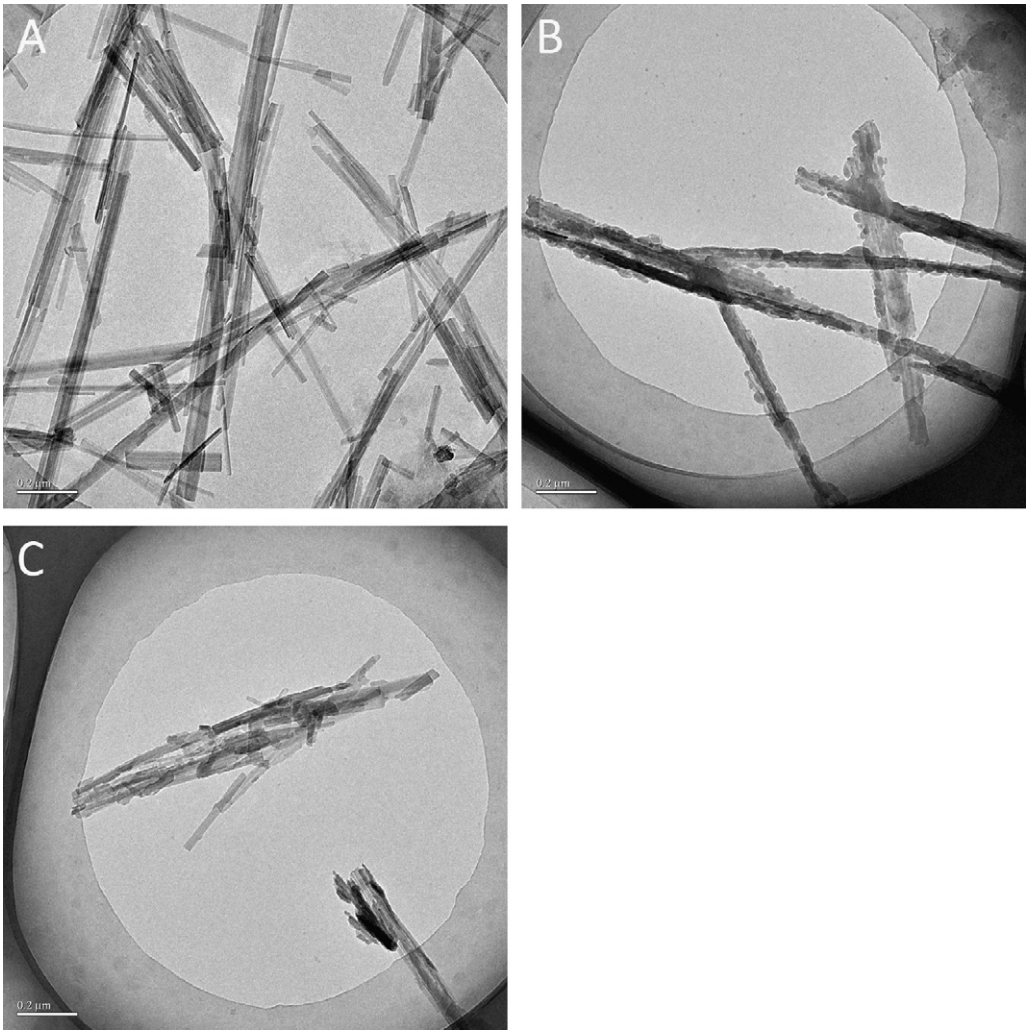

Fig. 6. TEM micrographs of pristine sepiolite and mercapto functionalized samples. (A) SEP; (B) MSEP-NT; (C) MSEP-GF.

physically bonded to sepiolite on the external surface and in the structural channels. A slight decreasing of the physically bonded water was observed with the modifier content in TG curves. This fact indicated a more hydrophobic nature of the surface of mercapto functionalized samples. However, the high specific surface area of the functionalized samples always retained water. The second weight loss region mainly related to the modifier decomposition. Pristine sepiolite lost two of the four coordinated crystallization water molecules at about 300 °C. In the temperature range of zeolitic water loss, the organic modifier was stable whereas the following dehydration steps overlap thermal volatilization of the modifier which was affected by the contact with the dehydrating sepiolite. This behavior which was observed for the organically modified sepiolite was due to the fact that part of the modifier molecules are physisorbed and degrade in the first step owing to catalytic effect of sepiolite [51]. The elimination of the other two molecules occurred at 525 °C. The DTG curves showed the removal of the water molecules in the functionalized samples. Meanwhile the low temperature removal of crystallization water overlapped with the modifier elimination, and the high temperature ones seemed quite similar in the different functionalized samples. The final step of the sepiolite weight losses corresponded to the removal of constitution water or hydroxyl groups around 750 °C.

3.3. Sorption of Pb(II) and Cd(II) on pristine sepiolite and mercapto functionalized samples

The maximum sorption capacities corresponding to MSEP-NT and MSEP-GF with Pb(II) and Cd(II) ions respectively are shown in Table 4. Additional data obtained from the literatures for analogous mercapto functionalized mesoporous or clays are also given for comparison. They are prepared either by chemical grafting on the surface of porous materials or natural clays or by a one-step synthesis through condensation of silane and silane couple

Table 3
Thermogravimetric analysis data of pristine sepiolite and mercapto functionalized samples.

Samples	25–150 °C		150–420 °C		420–650 °C		650–800 °C
	Mass (%)	T (°C)	Mass (%)	T (°C)	Mass (%)	T (°C)	Mass (%)
SEP	5.61	69	3.80	350	2.50	513	1.27
MSEP-NT	5.15	56	12.67	265; 357	8.77	500	1.44
MSEP-GF	3.74	60	9.66	276; 355	4.53	496	1.34

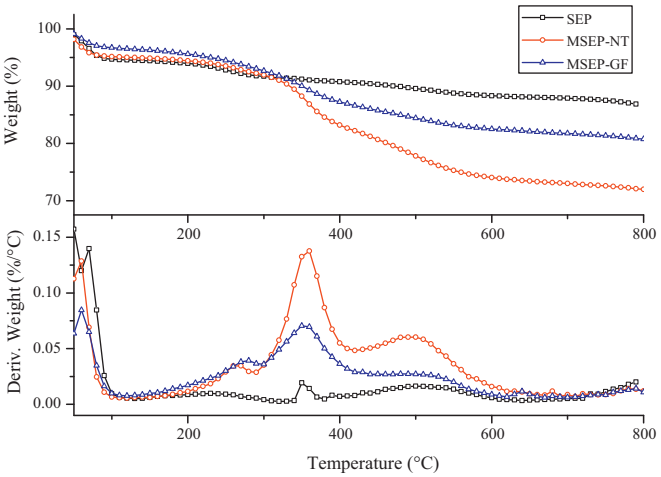

Fig. 7. TG/DTG of pristine sepiolite and mercapto functionalized samples in nitrogen atmosphere.

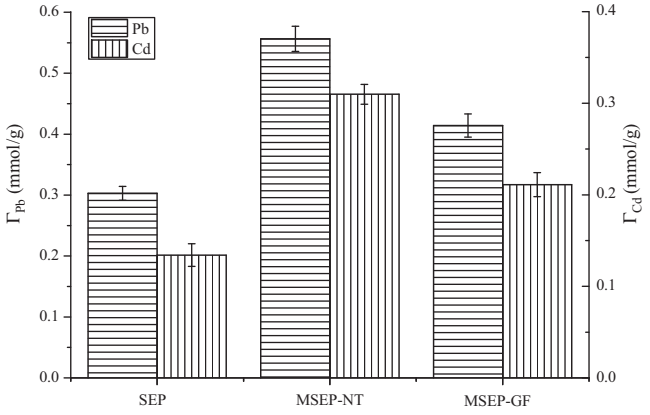

Fig. 8. Sorption capacities on pristine sepiolite and mercapto functionalized samples.

reagents. As shown in Table 4, mercapto functionalized sepiolite samples demonstrate a very high affinity for Pb(II) and Cd(II) ions. In the eleven kinds of adsorbents, mercapto functionalized magnesium phyllosilicate clay has the best performance, but in the preparation process, a great deal of methanol was needed. For MSEP-NT only natural sepiolite and mercapto silane were needed. The current work demonstrates that mercapto functionalized materials, prepared in a rapid, environmentally friendly and low-cost one-step synthesis that combines a high concentration of thiol binding sites with an expandable porous structure, exhibit the higher effectiveness ever observed for the capture of Pb(II), and Cd(II) ions.

The sorption capacities for Pb(II) and Cd(II) on pristine sepiolite were 0.30 and 0.13 mmol/g, respectively. After surface modification, the sorption capacities increased significantly. MSEP-NT and MSEP-GF can increase the sorption capacity of Pb(II) by 84.23% and 36.74%, meanwhile these for Cd(II) are 130.98% and 57.75% as shown in Fig. 8. Rapid color changes of mercapto functionalized samples from white to yellow were observed that occurred only a few minutes after the powder was contacted with Pb(II) solutions [15]. According to hard and soft acids and bases theory of Pearson [52], mercapto group is employed to modify the silica surface, due to its bonding ability with heavy metal ions such as Hg(II), Pb(II), Cd(II) and Cu(II). Cd(II) is not removed as efficiently as Pb(II), with weaker binding strength to mercapto functionalized sepiolite. The absolute hardness parameter of mercapto group as soft base is 4.1, while the parameters of Pb(II) and Cd(II) are 8.5 and 10.3, respectively. Soft metal ions are prone to forming stable complexation with ligands containing soft donor atoms. Sulfur can be regarded as a typical soft donor atom. Therefore, the functionalized sepiolite exhibits a high complexation affinity for the softer metal ion Pb(II), while low complexation affinity for harder Cd(II). The mercapto groups on the surface can react with heavy metal ions directly to form stable inner-sphere complexation via covalent binding and outer-sphere complexation through electrostatic binding reactions [53].

Suitable clay functionalization may improve the capacity and selectivity of clays as adsorbents of heavy metals and remedate soils and water contaminated by heavy metals. Additional experiments are currently underway to investigate the adsorption properties of mercapto functionalized sepiolite in simulated wastewaters and polluted soils containing heavy metals. The effects of variations in pH and ion strength on the sorption capacity and the thermodynamic parameters (ΔH^0, ΔS^0, and ΔG^0) are currently being studied. Further investigations will focus on increasing the accessible mercapto content and elucidating the detailed adsorption mechanism at molecular level.

Table 4
Comparison between maximum sorption capacities of different mercapto functionalized adsorbents.

Adsorbents samples	Sulfur content[a] (mmol/g)	Sorption capacity (mmol/g)	References
PCHs	–	Pb 0.11, Cd 0.22	[54]
Thiol-SAMMS	5.2	Pb 0.36, Cd 0.63	[55,56]
HBS-SH	3.27	Pb 0.57, Cd 0.30	[40]
Thiol-montmorillonite	3.2	Pb 0.35, Cd 0.24	[13]
Mg-MTMS	6.4	Pb 1.76, Cd 1.87	[15]
SH-mSi@Fe_3O_4	0.38	Pb 0.44	[57]
S-MCM-41	2.96	Pb 0.43	[58]
SH-MCM-41	2.61	Pb 0.49	[59]
Hybrid adsorbent MI	1.03	Pb 0.71	[60]
Hybrid adsorbent SN	1.19	Pb 1.17	[60]
H_1SiO_2-SH-10-HE	1.47	Cd 0.17	[61]
MSEP-NT	3.83	Pb 0.56, Cd 0.31	this work
MSEP-GF	1.72	Pb 0.31, Cd 0.21	this work

[a] The sulfur contents were determined by elemental analyses.

4. Conclusions

Mercapto functionalized sepiolite was prepared by nanotexturization in aqueous sepiolite gel and surface grafting in toluene with mercaptopropyltrimethoxysilane. The pristine sepiolite and mercapto functionalized samples were well characterized. The chemical bonding takes place between the surface hydroxyl group within sepiolite and the methoxy group of mercaptopropyltrimethoxysilane. The surface modification can increase the sorption capacities for Pb(II) and Cd(II). In term of operating simplicity and large scale production, nanotexturization is better than surface grafting in toluene. The results suggest mercapto functionalized sepiolite could provide a potential remedy for heavy metal contamination in soils and water.

Acknowledgements

This research was supported by the National High Technology Research and Development Program of China (no. 2008AA06Z334), National Natural Science Foundation of China (no. 40901154, 21107056 and 21177068), Natural Science Foundation of Tianjin (no. 10JCYBJC06300) and Central Public Research Institutes Basic Funds for Research and Development (Agro-Environmental Protection Institute, Ministry of Agriculture).

References

[1] H. Bradl, Adsorption of heavy metal ions on clays, in: P. Somasundaran, A. Hubbard (Eds.), Encyclopedia of Surface and Colloid Science, Taylor and Francis, New York, 2006, pp. 471–483.
[2] H.B. Bradl, Adsorption of heavy metal ions on soils and soils constituents, J. Colloid Interface Sci. 277 (2004) 1–18.
[3] M. Cruz-Guzmán, R. Celis, M.C. Hermosín, W.C. Koskinen, E.A. Nater, J. Cornejo, Heavy metal adsorption by montmorillonites modified with natural organic cations, Soil Sci. Soc. Am. J. 70 (2006) 215–221.
[4] L. Mercier, T.J. Pinnavaia, Heavy metal ion adsorbents formed by the grafting of a thiol functionality to mesoporous silica molecular sieves: factors affecting Hg(II) uptake, Environ. Sci. Technol. 32 (1998) 2749–2754.
[5] M. Jaber, J. Miehé-Brendlé, Organoclays: preparation, properties and applications, in: V. Valentin, M. Svetlana, T. Michael (Eds.), Ordered Porous Solids, Elsevier, Amsterdam, 2009, pp. 31–49.
[6] F. Wypych, Chemical modification of clay surfaces, in: P. Somasundaran, A. Hubbard (Eds.), Encyclopedia of Surface and Colloid Science, Taylor and Francis, New York, 2006, pp. 1256–1272.
[7] P. Stathi, K. Litina, D. Gournis, T.S. Giannopoulos, Y. Deligiannakis, Physicochemical study of novel organoclays as heavy metal ion adsorbents for environmental remediation, J. Colloid Interface Sci. 316 (2007) 298–309.
[8] P. Wu, W. Wu, S. Li, N. Xing, N. Zhu, P. Li, J. Wu, C. Yang, Z. Dang, Removal of Cd^{2+} from aqueous solution by adsorption using Fe-montmorillonite, J. Hazard. Mater. 169 (2009) 824–830.
[9] S.Z. Li, P.X. Wu, Characterization of sodium dodecyl sulfate modified iron pillared montmorillonite and its application for the removal of aqueous Cu(II) and Co(II), J. Hazard. Mater. 173 (2010) 62–70.
[10] Y. Deng, J.B. Dixon, G.N. White, Intercalation and surface modification of smectite by two non-ionic surfactants, Clays Clay Miner. 51 (2003) 150–161.
[11] N. Hüsing, Design of inorganic and inorganic-organic hybrid materials by sol-gel processing – from nanostructures to hierarchical networks, in: P. Innocenzi, Y.L. Zub, V.G. Kessler (Eds.), Sol-Gel Methods for Materials Processing, Springer, Berlin, 2008, pp. 91–104.
[12] Y. Cohen, V. Nguyen, J.-D. Jou, N. Bei, W. Yoshida, Surface modification of inorganic oxide surfaces by graft polymerization, in: J.A. Wingrave (Ed.), Oxide Surfaces, CRC Press, New York, 2001, pp. 321–353.
[13] C. Detellier, Preparation, characterization, and applications as heavy metals sortants of covalently grafted thiol functionalities on the interlamellar surface of montmorillonite, Environ. Sci. Technol. 29 (1995) 1318–1323.
[14] M. Jaber, J. Miehé-Brendlé, L. Michelin, L. Delmotte, Heavy metal retention by organoclays: synthesis, applications, and retention mechanism, Chem. Mater. 17 (2005) 5275–5281.
[15] I.L. Lagadic, M.K. Mitchell, B.D. Payne, Highly effective adsorption of heavy metal ions by a thiol-functionalized magnesium phyllosilicate clay, Environ. Sci. Technol. 35 (2001) 984–990.
[16] A. Alvarez, Sepiolite: properties and uses, in: A. Singer, E. Galan (Eds.), Developments in Sedimentology, Elsevier, Amsterdam, 1984, pp. 253–287.
[17] L. Bokobza, A. Burr, G. Garnaud, M.Y. Perrin, S. Pagnotta, Fibre reinforcement of elastomers: nanocomposites based on sepiolite and poly(hydroxyethyl acrylate), Polym. Int. 53 (2004) 1060–1065.
[18] E. Burzo, Sepiolite and palygorskite group of silicates, in: H.P.J. Wijn (Ed.), Phyllosilicates, Springer-Verlag, Berlin Heidelberg, 2009, pp. 340–403.
[19] D. García-López, J.F. Fernández, J.C. Merino, J. Santarén, J.M. Pastor, Effect of organic modification of sepiolite for PA 6 polymer/organoclay nanocomposites, Compos. Sci. Technol. 70 (2010) 1429–1436.
[20] M.C. Hermosin, J. Cornejo, Methylation of sepiolite and palygorskite with diazomethane, Clays Clay Miner. 34 (1986) 591–596.
[21] N. Garciĩa, J. Guzmaĩn, E. Benito, A. Esteban-Cubillo, E. Aguilar, J. Santareĩn, P. Tiemblo, Surface modification of sepiolite in aqueous gels by using methoxysilanes and its impact on the nanofiber dispersion ability, Langmuir 27 (2011) 3952–3959.
[22] R. Celis, M. Carmen Hermosín, J. Cornejo, Heavy metal adsorption by functionalized clays, Environ. Sci. Technol. 34 (2000) 4593–4599.
[23] R.P. Hodgkins, A.E. Garcia-Bennett, P.A. Wright, Structure and morphology of propylthiol-functionalised mesoporous silicas templated by non-ionic triblock copolymers, Microporous Mesoporous Mater. 79 (2005) 241–252.
[24] J.P. Badyal, A.M. Cameron, N.R. Cameron, D.M. Coe, R. Cox, B.G. Davis, L.J. Oates, G. Oye, P.G. Steel, A simple method for the quantitative analysis of resin bound thiol groups, Tetrahedron Lett. 42 (2001) 8531–8533.
[25] B.G. Trewyn, H.-T. Chen, V.S.Y. Lin, Surface-functionalized nanoporous catalysts for renewable chemistry, in: M. Benaglia (Ed.), Recoverable and Recyclable Catalysts, John Wiley and Sons Ltd., Chichester, 2009, pp. 15–47.
[26] M.C. Brochier Salon, M.N. Belgacem, Competition between hydrolysis and condensation reactions of trialkoxysilanes, as a function of the amount of water and the nature of the organic group, Colloids Surf., A 366 (2010) 147–154.
[27] C. Wan, B. Chen, Synthesis and characterization of biomimetic hydroxyapatite/sepiolite nanocomposites, Nanoscale 3 (2011) 693–700.
[28] V. Marjanovic, S. Lazarevic, I. Jankovic-Castvan, B. Potkonjak, Đ. Janackovic, R. Petrovic, Chromium (VI) removal from aqueous solutions using mercaptosilane functionalized sepiolites, Chem. Eng. J. 166 (2011) 198–206.
[29] H. Chen, M. Zheng, H. Sun, Q. Jia, Characterization and properties of sepiolite/polyurethane nanocomposites, Mater. Sci. Eng., A 445-446 (2007) 725–730.
[30] C. Giles, T. MacEwan, S. Nakhwa, D. Smith, Studies in adsorption. Part XI. A system of classification of solution adsorption isotherms, and its use in diagnosis of adsorption mechanisms and in measurement of specific surface areas of solids, J. Chem. Soc. 3 (1960) 3973–3993.
[31] E. Ruiz-Hitzky, Molecular access to intracrystalline tunnels of sepiolite, J. Mater. Chem. 11 (2001) 86–91.
[32] S. Lazarević, I. Janković-Častvan, D. Jovanović, S. Milonjić, D. Janaćković, R. Petrović, Adsorption of Pb^{2+}, Cd^{2+} and Sr^{2+} ions onto natural and acid-activated sepiolites, Appl. Clay Sci. 37 (2007) 47–57.
[33] J.L. Ahlrichs, C. Serna, J.M. Serratosa, Structural hydroxyls in sepiolites, Clays Clay Miner. 23 (1975) 119–124.
[34] M. Doğan, Y. Turhan, M. Alkan, H. Namli, P. Turan, Ö. Demirbaş, Functionalized sepiolite for heavy metal ions adsorption, Desalination 230 (2008) 248–268.
[35] H. Chen, D. Zeng, X. Xiao, M. Zheng, C. Ke, Y. Li, Influence of organic modification on the structure and properties of polyurethane/sepiolite nanocomposites, Mater. Sci. Eng., A 528 (2011) 1656–1661.
[36] C. Che, T.D. Glotch, D.L. Bish, J.R. Michalski, W. Xu, Spectroscopic study of the dehydration and/or dehydroxylation of phyllosilicate and zeolite minerals, J. Geophys. Res. 116 (2011) E05007.
[37] Y. Turhan, P. Turan, M. Doğan, M. Alkan, H. Namli, O. Demirbaş, Characterization and adsorption properties of chemically modified sepiolite, Ind. Eng. Chem. Res. 47 (2008) 1883–1895.
[38] M.A. Vicente, M. Suaĩrez, J.D.D. Loĩpez-Gonzaĩlez, M.A. Bañares-Muñoz, Characterization, surface area, and porosity analyses of the solids obtained by acid leaching of a saponite, Langmuir 12 (1996) 566–572.
[39] R.L. Frost, E. Mendelovici, Modification of fibrous silicates surfaces with organic derivatives: an infrared spectroscopic study, J. Colloid Interface Sci. 294 (2006) 47–52.
[40] X. Liang, Y. Xu, G. Sun, L. Wang, Y. Sun, X. Qin, Preparation, characterization of thiol-functionalized silica and application for sorption of Pb^{2+} and Cd^{2+}, Colloids Surf., A 349 (2009) 61–68.
[41] M.A. Aramendía, V. Borau, C. Jiménez, J.M. Marinas, J.R. Ruiz, Characterization of Spanish sepiolites by high-resolution solid-state NMR, Solid State Nucl. Magn. Reson. 8 (1997) 251–256.
[42] B. Hubbard, W. Kuang, A. Moser, G.A. Facey, C. Detellier, Structural study of Maya Blue: textural thermal and solid-state multinuclear magnetic resonance characterization of the palygorskite-indigo and sepiolite-indigo adducts, Clays Clay Miner. 51 (2003) 318–326.
[43] I. Dékány, L. Turi, A. Fonseca, J.B. Nagy, The structure of acid treated sepiolites: small-angle X-ray scattering and multi MAS-NMR investigations, Appl. Clay Sci. 14 (1999) 141–160.
[44] J.L. Valentín, M.A. López-Manchado, P. Posadas, A. Rodríguez, A. Marcos-Fernández, L. Ibarra, Characterization of the reactivity of a silica derived from acid activation of sepiolite with silane by ^{29}Si and ^{13}C solid-state NMR, J. Colloid Interface Sci. 298 (2006) 794–804.
[45] W. Kuang, G.A. Facey, C. Detellier, Organo-mineral nanohybrids. Incorporation, coordination and structuration role of acetone molecules in the tunnels of sepiolite, J. Mater. Chem. 16 (2006) 179–185.
[46] N. Garciĩa, E. Benito, J. Guzmaĩn, R. de Francisco, P. Tiemblo, Microwave versus conventional heating in the grafting of alkyltrimethoxysilanes onto silica particles, Langmuir 26 (2010) 5499–5506.
[47] N. García, E. Benito, J. Guzmán, P. Tiemblo, Use of p-toluenesulfonic acid for the controlled grafting of alkoxysilanes onto silanol containing surfaces: preparation of tunable hydrophilic, hydrophobic, and super-hydrophobic silica, J. Am. Chem. Soc. 129 (2007) 5052–5060.
[48] M.R. Weir, W. Kuang, G.A. Facey, C. Detellier, Solid-state nuclear magnetic resonance study of sepiolite and partially dehydrated sepiolite, Clays Clay Miner. 50 (2002) 240–247.
[49] H. Nagata, S. Shimoda, T. Sudo, On dehydration of bound water of sepiolite, Clays Clay Miner. 22 (1974) 285–293.
[50] R. Frost, J. Kristóf, E. Horváth, Controlled rate thermal analysis of sepiolite, J. Therm. Anal. Calorim. 98 (2009) 749–755.
[51] G. Tartaglione, D. Tabuani, G. Camino, Thermal and morphological characterisation of organically modified sepiolite, Microporous Mesoporous Mater. 107 (2008) 161–168.
[52] R.G. Pearson, Hard soft acids and bases, J. Am. Chem. Soc. 85 (1963) 3533–3539.
[53] D.L. Sparks, Sorption phenomena on soils, in: D.L. Sparks (Ed.), Environmental Soil Chemistry, Elsevier Science, San Diego, 2003, pp. 133–186.
[54] R. Tassanapayak, R. Magaraphan, H. Manuspiya, Functionalized porous clay heterostructure for heavy metal adsorption from wastewater, Adv. Mater. Res. 55-57 (2008) 617–620.
[55] X. Feng, G.E. Fryxell, L.Q. Wang, A.Y. Kim, J. Liu, K.M. Kemner, Functionalized monolayers on ordered mesoporous supports, Science 276 (1997) 923–926.
[56] M. Shas, F. Glen, P. Kent, L. Yuehe, Application of novel nanoporous sorbents for the removal of heavy metals, metalloids, and radionuclides, in: M.N.V. Prasad, K.S. Sajwan, R. Naidu (Eds.), Trace Elements in the Environment: Biogeochemistry, Biotechnology and Bioremediation, CRC Press, Boca Raton, 2005, pp. 369–380.
[57] G. Li, Z. Zhao, J. Liu, G. Jiang, Effective heavy metal removal from aqueous systems by thiol functionalized magnetic mesoporous silica, J. Hazard. Mater. 192 (2011) 277–283.
[58] S.A. Idris, C.M. Davidson, C. McManamon, M.A. Morris, P. Anderson, L.T. Gibson, Large pore diameter MCM-41 and its application for lead removal from aqueous media, J. Hazard. Mater. 185 (2011) 898–904.

[59] S. Wu, F. Li, R. Xu, S. Wei, G. Li, Synthesis of thiol-functionalized MCM-41 mesoporous silicas and its application in Cu(II), Pb(II), Ag(I), and Cr(III) removal, J. Nanopart. Res. 12 (2010) 2111–2124.
[60] C.A. Quirarte-Escalante, V. Soto, W. de la Cruz, G.R. Porras, R. Manrïíquez, S. Gomez-Salazar, Synthesis of hybrid adsorbents combining sol-gel processing and molecular imprinting applied to lead removal from aqueous streams, Chem. Mater. 21 (2009) 1439–1450.
[61] D. Liu, J.-H. Lei, L.-P. Guo, X.-D. Du, K. Zeng, Ordered thiol-functionalized mesoporous silica with macrostructure by true liquid crystal templating route, Microporous Mesoporous Mater. 117 (2009) 67–74.